

# Interaction of the copper chaperone HAH1 with the Wilson disease protein is essential for copper homeostasis

Iqbal Hamza, Mark Schaefer, Leo W. J. Klomp, and Jonathan D. Gitlin\*

Edward Mallinckrodt Department of Pediatrics, Washington University School of Medicine, St. Louis, MO

Edited by Stuart A. Kornfeld, Washington University School of Medicine, St. Louis, MO, and approved September 16, 1999 (received for review July 7, 1999)

**The delivery of copper to specific sites within the cell is mediated by distinct intracellular carrier proteins termed copper chaperones. Previous studies in *Saccharomyces cerevisiae* suggested that the human copper chaperone HAH1 may play a role in copper trafficking to the secretory pathway of the cell. In this current study, HAH1 was detected in lysates from multiple human cell lines and tissues as a single-chain protein distributed throughout the cytoplasm and nucleus. Studies with a glutathione S-transferase-HAH1 fusion protein demonstrated direct protein-protein interaction between HAH1 and the Wilson disease protein, which required the cysteine copper ligands in the amino terminus of HAH1. Consistent with these *in vitro* observations, coimmunoprecipitation experiments revealed that HAH1 interacts with both the Wilson and Menkes proteins *in vivo* and that this interaction depends on available copper. When these studies were repeated utilizing three disease-associated mutations in the amino terminus of the Wilson protein, a marked diminution in HAH1 interaction was observed, suggesting that impaired copper delivery by HAH1 constitutes the molecular basis of Wilson disease in patients harboring these mutations. Taken together, these data provide a mechanism for the function of HAH1 as a copper chaperone in mammalian cells and demonstrate that this protein is essential for copper homeostasis.**

Copper is an essential micronutrient that plays a critical role in the biochemistry of all aerobic organisms (1). The reactivity of copper in biological systems also accounts for the toxicity of this metal, which results from the rapid generation of reactive oxygen species when copper homeostasis is impaired (2). These concepts are illustrated by the genetic disorders of copper transport, Menkes and Wilson disease, which underscore the essential need for copper as well as the toxicity of this metal (3). Despite strikingly different clinical phenotypes, each disease results from absence or dysfunction of homologous copper-transporting ATPases located in the trans-Golgi network of cells. Elucidation of the molecular basis of these diseases indicates that specific mechanisms have evolved that direct the trafficking of copper into the secretory pathway of the cell for subsequent incorporation into proteins and excretion.

A series of genetic studies in *Saccharomyces cerevisiae* has revealed that the delivery of copper to specific cellular pathways is mediated by a group of proteins termed copper chaperones (4). ATX1 encodes a cytosolic copper-binding protein originally identified as a multicopy suppressor of *sod1Δ* mutants (5). Atx1p contains a single repeat of the MXCXXC copper-binding motif present in the Wilson and Menkes proteins and functions to deliver copper to the secretory pathway for the biosynthesis of Fet3Pp, a multicopper oxidase required for high-affinity iron uptake in this organism (6, 7). Atx1p has been highly conserved through evolution, and homologous sequences have been identified in flies, worms, and plants (8–10). HAH1 is a 68-aa protein identified as a human homologue of Atx1p. This protein has been shown to functionally complement *atx1Δ* mutant strains, suggesting that HAH1 may play a role in copper homeostasis in mammalian cells (11, 12).

Previous studies using a yeast two-hybrid system revealed that Atx1p can interact with the amino terminus of Ccc2p, the yeast homologue of the Wilson and Menkes proteins (13). These findings suggested a potential mechanism for copper delivery to the secretory pathway that is supported by more recent data on the structures of HAH1 (12) and Atx1p (14, 15), which reveal a remarkable conservation with the NMR solution structure of a single copper-binding domain of the Menkes protein (16). Nevertheless, despite these experiments in yeast, the function of HAH1 remains unknown. This current study was undertaken to critically examine the distribution and interactions of HAH1 in mammalian cells and to elucidate the physiological role of this protein in cellular copper homeostasis.

## Materials and Methods

**Cell Culture, Tissues, and Antibodies.** Cell lines were obtained and cultured as described previously (11). Human tissues were obtained at autopsy under the guidelines of the Human Studies Committee of the Washington University School of Medicine, St. Louis, MO. (Institutional Review Board 94–0909). A murine monoclonal antibody to the Flag epitope (M2) was purchased from Sigma. Affinity-purified antiserum to the Wilson and Menkes proteins was as described previously (17, 18). To generate HAH1 antibody, oligonucleotide primers were synthesized and used to amplify a full-length human HAH1 cDNA (11). The resulting cDNA fragment was ligated into pGEX4T and purified from *Escherichia coli* BL21(DE3) cells harboring the expression plasmid (19). Bound glutathione S-transferase (GST) fusion protein was eluted with 10 mM reduced glutathione in 50 mM Tris-HCl, pH 8.0, dialyzed, resuspended, and cleaved with thrombin. Purified HAH1 protein was used to produce polyclonal antisera in rabbits (Animal Pharm Services, Healdsburg, CA). HAH1 antisera was affinity purified against recombinant HAH1 protein by using polyvinylidene difluoride membranes (20).

**Subcloning, Mutagenesis, and *in Vitro* Translation.** To generate epitope-tagged HAH1, HAH1 cDNA was amplified and ligated into the *NotI* and *BamHI* sites of pFlagCMV2 (Kodak). Site-directed mutagenesis of the human Wilson cDNA in pCDNA3.1 was performed by using KlenTaq polymerase and oligonucleotide primer pairs corresponding to the G85V, L492S, and G591D mutations (21). The sequence of all constructs was confirmed by dideoxy nucleotide sequencing. Wild-type and mutant Wilson cDNAs in pCDNA3.1 were transcribed and translated *in vitro* in the presence of T7 polymerase, rabbit reticulocyte lysate, and 20

This paper was submitted directly (Track II) to the PNAS office.

Abbreviations: GST, glutathione S-transferase; BCS, bathocuproine disulfonic acid; DAPI, 4',6-diamidino-2-phenylindole.

\*To whom reprint requests should be addressed at: St. Louis Children's Hospital, One Children's Place, St. Louis, MO 63110. E-mail: gitlin@kids.wustl.edu.

The publication costs of this article were defrayed in part by page charge payment. This article must therefore be hereby marked "advertisement" in accordance with 18 U.S.C. §1734 solely to indicate this fact.

$\mu\text{Ci}$  of [ $^{35}\text{S}$ ]methionine and [ $^{35}\text{S}$ ]cysteine by using a TNT kit (Promega) according to the manufacturer's specifications. Before interaction studies, one-twentieth of the total reaction was analyzed by SDS/PAGE for quantitation by PhosphorImager (Molecular Dynamics). Equivalent amounts of [ $^{35}\text{S}$ ]Wilson protein were then used for GST interaction analysis as described below.

**Cell Transfection, Immunoblotting, and Immunofluorescence.** Transient transfections were performed with lipofectamine (GIBCO/BRL) according to manufacturer's instructions. Tissue lysates were frozen and homogenized in liquid nitrogen, heated at  $100^\circ\text{C}$  for 10 min in the presence of SDS sample buffer containing  $\beta$ -mercaptoethanol, and centrifuged for 15 min at  $16,000 \times g$  at  $4^\circ\text{C}$  before the supernatant for immunoblotting was removed. Cells were lysed in 50 mM Hepes/0.1% Nonidet P-40/250 mM NaCl supplemented with protease inhibitors, followed by centrifugation for 15 min at  $6,000 \times g$  at  $4^\circ\text{C}$ . Protein concentration for all samples was determined by the method of Bradford (22). For immunoblotting, proteins were separated by SDS/PAGE, transferred to nitrocellulose, and detected by chemiluminescence as described previously (17).

For indirect immunofluorescence, cells were grown on glass coverslips, fixed in 4% paraformaldehyde, and permeabilized in 0.2% Triton-X 100, as described (17). In some experiments, cells were preincubated in either 50  $\mu\text{M}$  bathocuproine disulfonic acid (BCS) for 16–24 hr or 400  $\mu\text{M}$   $\text{CuCl}_2$  for 2–3 hr. After staining with secondary antibodies conjugated with fluorescein isothiocyanate or tetramethylrhodamine isothiocyanate, coverslips were mounted and analyzed by using an Olympus BX-60 microscope. Through-focus images were obtained by using a laser scanning confocal microscope as described previously (18). For nuclear staining, HAH1-labeled HeLa cells were incubated with 2 ng/ $\mu\text{l}$  of 4',6-diamidino-2-phenylindole (DAPI) for 4 min before mounting and visualized with a Standard Chroma narrow-band UV set.

**Immunoprecipitation and GST-Binding Assay.** For coimmunoprecipitation studies, cells were incubated with 200  $\mu\text{M}$   $\text{CuCl}_2$  or 50  $\mu\text{M}$  BCS for 12 hr before lysis. Cells were lysed in 50 mM MOPS, pH 6.8/0.1% Nonidet P-40/250 mM NaCl/protease inhibitors supplemented with either 5 mM DTT and 1 mM  $\text{CuCl}_2$  or 1 mM BCS. Cu-DTT or BCS was maintained through all subsequent steps. Cell debris was pelleted for 15 min at  $6,000 \times g$  at  $4^\circ\text{C}$ , and 750  $\mu\text{g}$  of this lysate was utilized for immunoprecipitation and subsequent immunoblotting as described previously (23). For some experiments, cells were pulse labeled for 2 hr with 300  $\mu\text{Ci}/\text{ml}$  of [ $^{35}\text{S}$ ]methionine and [ $^{35}\text{S}$ ]cysteine and chased for periods up to 72 hr followed by immunoprecipitation as described (17). In all cases, the protein concentration of the precleared supernatant was determined, and equivalent amounts of protein were immunoprecipitated with the HAH1, Wilson, or Menkes antisera.

Glutathione-agarose beads (25  $\mu\text{l}$ ), pretreated with 25  $\mu\text{g}/\text{ml}$  polyvinylpyrrolidone -130 and 25  $\mu\text{g}/\text{ml}$  casein to decrease nonspecific binding, were incubated at  $4^\circ\text{C}$  for 30 min with 50 pmol of purified GST proteins in 250  $\mu\text{l}$  of binding buffer containing PBS, pH 7.4, 1 mM DTT, 0.5% Triton-X 100, 0.5% Nonidet P-40, 0.5 mM PMSF, and 100  $\mu\text{g}$  of BL21 (DE3) lysate. COS-7 cells expressing the Wilson cDNAs were preincubated for 1 hr in 1 mM  $\text{CuCl}_2$ , lysed in 50 mM Hepes, pH 7.4/250 mM NaCl/1% Nonidet P-40/1% Triton X-100/protease inhibitors and centrifuged for 15 min at  $6,000 \times g$  at  $4^\circ\text{C}$ . COS-7 lysates (150  $\mu\text{g}$ ) were then incubated with GST fusion protein beads for 1 hr at  $4^\circ\text{C}$  followed by washes with 6 ml binding buffer containing 250 mM NaCl. Bound proteins were eluted at  $37^\circ\text{C}$  for 10 min in the presence of 30  $\mu\text{l}$  of SDS sample buffer containing  $\beta$ -mercaptoethanol. For some experiments, the GST-binding

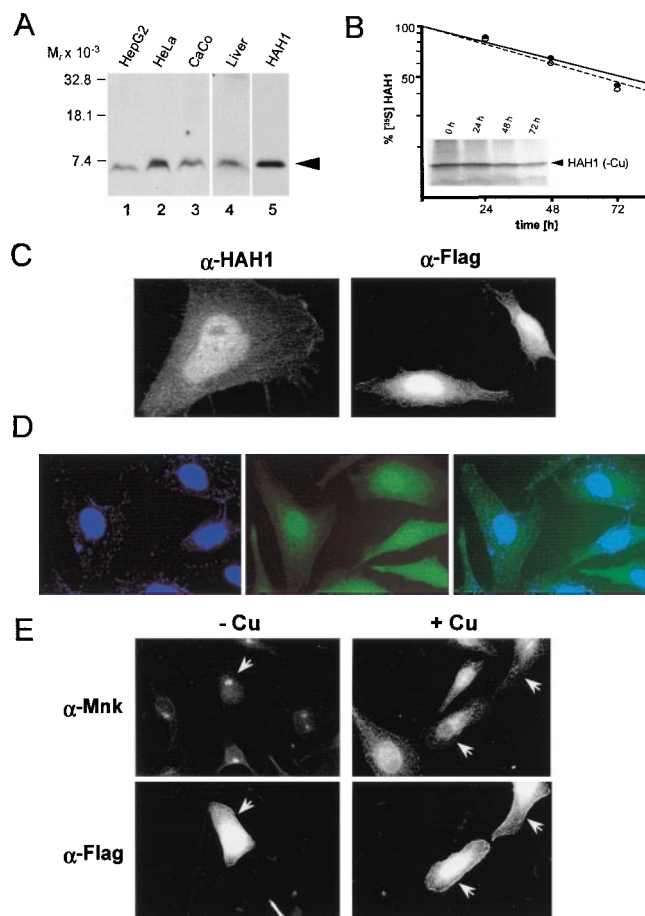


**Fig. 1.** (A) Immunoblot analysis with HAH1 antibody. Protein lysates (100  $\mu\text{g}$ ) (lanes 1–4) or 100 ng of recombinant HAH1 expressed in *E. coli* (lane 5) was separated by SDS/PAGE on 10–20% Tricine gradient gels, transferred to nitrocellulose, and analyzed by chemiluminescence. (B) HeLa cells grown in the presence of BCS (●) or copper (○) were lysed and immunoprecipitated with HAH1 antisera. Following a 2-hr pulse with [ $^{35}\text{S}$ ]methionine and [ $^{35}\text{S}$ ]cysteine, cells were lysed and immunoprecipitated at indicated chase times followed by SDS/PAGE, autoradiography, and quantitation of bands. (Inset) HAH1 immunoprecipitated in the presence of BCS. (C) Immunofluorescent localization of HAH1 in HeLa cells incubated with HAH1 antisera ( $\alpha$ -HAH1; confocal 100X) and Flag M2 antibody ( $\alpha$ -Flag; 60X). (D) Immunofluorescence of HeLa cells stained for nucleus with DAPI (narrow-band UV), HAH1 antiserum (FITC), or overlay images of DAPI and HAH1. (E) Double immunofluorescence in transfected HeLa cells treated with BCS (–Cu) or copper (+Cu) followed by incubation with Menkes ( $\alpha$ -Mnk) and Flag-M2 ( $\alpha$ -Flag) antibodies. Arrows indicate transfected HeLa cells.

assay was performed with 75  $\mu\text{l}$  of blocked beads incubated with 3 nmol of GST or GST-HAH1 in the presence of HepG2 or COS-7 cell lysate expressing the Wilson protein, followed by washes and elution of the bound proteins as described above. For *in vitro* translated proteins, radiolabeled protein bound to the glutathione columns was eluted, separated by SDS/PAGE, and analyzed and quantified by PhosphorImager.

## Results

As can be seen in Fig. 1A, a single polypeptide was detected in cell and tissue lysates analyzed by immunoblotting with an antibody specific to HAH1. The protein migrated at the same position as recombinant HAH1 expressed in *E. coli* (Fig. 1A, lane 5), albeit more rapidly than its predicted molecular mass of 7.4 kDa in SDS/PAGE. This band was not observed with preimmune sera or HAH1 antisera preincubated with the

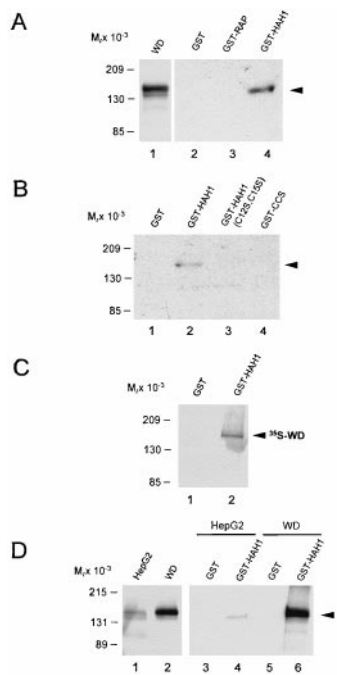


**Fig. 2.** *In vitro* interaction of HAH1 and Wilson protein. (A) COS-7 cell lysates (150  $\mu$ g) expressing Wilson protein (5  $\mu$ g; lane 1) were incubated with 50 pmol of purified GST-fusion proteins (lanes 2–4), and eluates were subjected to SDS/PAGE, transferred to nitrocellulose, and examined by immunoblotting with Wilson antisera. (B) COS-7 cell lysates expressing the Wilson protein were incubated with the indicated GST constructs (lanes 1–4) and analyzed as indicated above. (C) Full length Wilson cDNA was translated *in vitro* in the presence of [ $^{35}$ S]methionine and [ $^{35}$ S]cysteine followed by incubation with the GST constructs as indicated. Interacting proteins were separated by SDS/PAGE and analyzed by autoradiography. (D) One milligram of HepG2 cell lysate (100  $\mu$ g; lane 1) or 150  $\mu$ g COS-7 cell lysate expressing the Wilson protein (5  $\mu$ g; lane 2) was incubated with 3 nmol of purified GST fusion proteins (lanes 3–6) and analyzed by immunoblotting with Wilson antisera as before.

HAH1-GST fusion protein (data not shown). To further characterize HAH1, HeLa cells were pulse labeled with [ $^{35}$ S]methionine and [ $^{35}$ S]cysteine, and at specific chase periods cell lysates were immunoprecipitated and subjected to SDS/PAGE. These biosynthetic studies revealed that HAH1 is synthesized as a single peptide with a  $t_{1/2}$  of 72 hr, which was unaffected by the intracellular copper concentration (Fig. 1B). In addition, the relative abundance of HAH1 in HeLa cells was unaffected by changes in the intracellular concentration of iron, cobalt, nickel, or zinc (data not shown).

Immunofluorescent microscopy was performed to determine the intracellular location of HAH1. These studies detected HAH1 throughout the cytoplasm and nucleus of HeLa cells (Fig. 1C). The distribution of HAH1 detected with the polyclonal antisera was specific as an identical pattern was observed when HeLa cells transiently transfected with epitope tagged HAH1 were examined utilizing an epitope-specific monoclonal antibody (Fig. 1C). The nuclear localization of HAH1 was confirmed by staining HAH1-immunolabeled HeLa cells with DAPI, which revealed consistent overlap of signals for HAH1 and the nucleus in these cells (Fig. 1D). Digitonin permeabilization of HeLa cells before immunofluorescence resulted in a complete loss of HAH1 signal, suggesting that this protein was not contained within cellular organelles (data not shown). Similar observations were made in multiple other cell lines where no overlap was observed when double immunofluorescent studies were performed utilizing antibodies for proteins known to be localized in

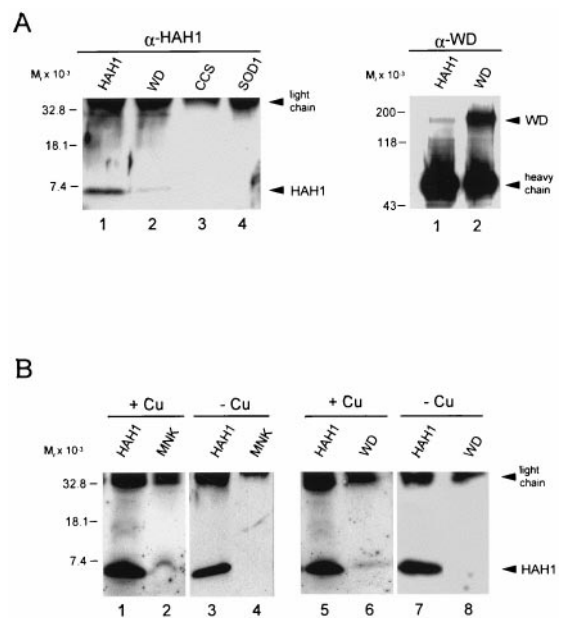


**Fig. 3.** (A) HepG2 cells were immunoprecipitated with either HAH1, Wilson, CCS, or SOD1 antisera, and the immunoprecipitates were separated by SDS/PAGE transferred to nitrocellulose and examined by immunoblotting with HAH1 ( $\alpha$ -HAH1) or Wilson ( $\alpha$ -WD) antisera. (B) HeLa and HepG2 cells grown in the presence of 200  $\mu$ M copper (lanes 1, 2 and 5, 6) or 50  $\mu$ M BCS (lanes 3, 4 and 7, 8) were immunoprecipitated with HAH1 (lanes 1, 3, 5, 7), Menkes (lanes 2, 4) or Wilson (lanes 6, 8) antisera. Immunoprecipitates were analyzed with HAH1 antisera as indicated above. IgG heavy and light chains detected by anti-rabbit secondary antibody are indicated.

the endoplasmic reticulum, trans-Golgi network, plasma membrane, or mitochondria (data not shown).

To examine the effect of copper on the intracellular localization of HAH1, double immunofluorescent studies were performed in HeLa cells transfected with an epitope-tagged HAH1 construct. As can be seen in Fig. 1E, alteration of the intracellular copper concentration by incubation of cells in media containing either the copper chelator BCS or excess Cu resulted in the expected translocation of the Menkes protein from the trans-Golgi network to a cytoplasmic vesicular compartment with increasing copper concentration (24). In contrast, these alterations in copper context had no effect on the intracellular distribution of HAH1 in these same cells (Fig. 1E). The failure to observe an effect of copper on HAH1 localization was not caused by the epitope tag, because the distribution of endogenous HAH1 was also unaffected by the cellular copper status in cells treated in this same fashion (data not shown).

The localization of HAH1 in the cytoplasm would permit this protein to deliver copper to the secretory pathway via interaction with the amino terminus of the copper-transporting ATPases. To investigate this possibility, column-binding assays were performed by utilizing a GST-HAH1 fusion protein. GST-HAH1 was immobilized on glutathione-agarose beads and mixed with cell lysates from COS-7 cells transiently transfected with a full length Wilson cDNA. After incubation, eluates were subjected to SDS/PAGE and analyzed by immunoblotting with a polyclonal antiserum to the Wilson protein. The Wilson protein was readily detected by this analysis in lysates of transfected cells (Fig. 2A, lane 1), and this protein was retained after incubation of these same lysates with GST-HAH1 (Fig. 2A, lane 4). The interaction of HAH1 with the Wilson protein was specific, because no protein was recovered after incubation of these cell lysates with GST or GST-RAP, a 39-kDa chaperone implicated

**A**

```

HAH1      ---MPKHEFSVD-MTCGGCAEAVSRVNLKLGGVK-YDIDLPNKKVCIESEHSMDTLLATLKKTKGTVSYLGL 68
WDCu1    -SSQVATSTVRILGMCQSCVKSIEDRISNLEGIISMKVSLEQDSATVKYVPSVVCLOQ-VCHIGDMGFEASI 125
WDCu2    -PAQEAVVKLRVEGMCQSCVSSIEGKVRKLGQVVRVKVSLSNQEAIVTYQPYLIQPED-LRDHVNDMGFEAAI 210
WDCu3    -GSHVVTLQLRIDGMHCKSCVNLNIEENIGQLLGVQS IQVSLNKTAVKYPSPCTS PVA-LQRAIEALPFGNFK 325
WDCu4    -QGTCSSTLIALAGMTCASCVHSIEGMISQLEGVQQISVSLAEGTATVLYNPSVISPEE-LRAAIEDMGFEASV 426
WDCu5    -AVAPQKCFIQIKGMCASCVSNIERNLQKEA VLSVLVALMAGKAEIKYDPEVIQPLE-IAQFIQDLGFEAAV 555
WDCu6    -AGSDGNIELTITGMCASCVHNIESKLRTRNGITYASVALATSKALVKDFPEIIGPRD-IIKIIEEIGFHASL 631

MKCu1    -SMGVNSVTISVEGMCNSCVWVTEQQIKGVNGVHHIKVSLSEKNATI IYDPRKLTPTK-LQEAIDDMGFDAVI 75
MKCu2    -QAGEVVLKMKVEGMCCHSCTSTIEGKIGKLGQVQRIVKVS LDNQEATI VYQPHLISVEE-MKKQIEAMGFPAFV 238
MKCu3    -YTNDSTATFIIDGMHCKSCVSNIESTLSALQVYSSIVVSLNRS AIVKYNASSVTPES-LRKAIVAVSPGLYR 344
MKCu4    -QPLTQETVINIDGMCNSCVQSIIEGVI SKKPGVKS IRVSLANSNGTVEYDPLLTSPET-LRGAIEDMGFDATL 444
MKCu5    -GKNSSKCYIQVTGMCASCVANIERNLRREEGIYSILVALMAGKAEVRYNPAVIQPPM-IAEFIRELGFQATV 555
MKCu6    DEG-DGVLLELVVRGMCASCVHKIESLTKHRGILYCSVALATNKAHIKYDPEIIGPRD-IIHTIESLGFEASL 631

RAN1Cu1  -VSGLRKIQVGVGMCACACNSVNEAALMNVNVEFKASVALLQNRADVDFPNLVKEED-IKEAIEDAGFEAEI 123
RAN1Cu2  -TQATLVGQFTIGGMCACACVNSVEGILRDLRPGVKRAVVALSTLSGVEVYDPNVINKDD-IVNAIEDAGFEGL 200
  
```

**B**

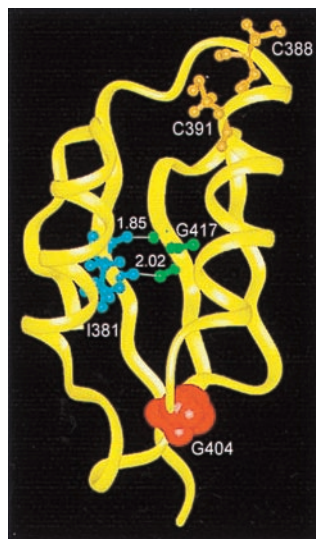


**Fig. 4.** (A) Amino acid sequence alignment of HAH1 and the copper-binding domains of the Wilson (WD), Menkes (MK), and RAN-1 proteins. The conserved MXCXXC motif and glycine residue are outlined. The Wilson disease mutations (G85V, L492S and G591D) are highlighted, and the RAN-1Cu2 mutation (G173E) noted by asterisk. (B) Structural model (Insight II, Molecular Simulations) of the Menkes fourth copper-binding domain on the basis of the NMR structure (16) depicting the relative positions of the Wilson protein and RAN-1 mutations. C388 and C391 are the copper-binding cysteines. Hydrogen bonds (Å) between I381 and G417 in an antiparallel  $\beta$ -sheet of the Menkes protein are indicated and correspond to L492 in the Wilson protein and G173 in RAN-1, respectively. G404 is shown with van der Waals surface and corresponds to the G85 and G591 Wilson protein mutations.

in low density lipoprotein receptor trafficking (Fig. 2A, lanes 2 and 3).

To examine the role of copper in this interaction, the column-binding assays were repeated by using HAH1 with mutations in two cysteine residues (C12S, C15S) essential for HAH1 copper binding (12). Elimination of these copper ligands completely abrogated the interaction between HAH1 and the Wilson protein, suggesting that copper may be essential for this process (Fig. 2B, lanes 2 and 3). This interaction between the Wilson protein and HAH1 did not depend simply on the MXCXXC motif in HAH1, because no interaction was detected when these same experiments were performed with the copper chaperone CCS, which also contains a single MXCXXC motif near the amino terminus (25) (Fig. 2B, lane 4). This interaction was direct and not mediated by additional components in the COS cell lysate, because incubation of GST-HAH1 with *in vitro*-translated Wilson protein also resulted in specific retention of this protein (Fig. 2C). The interaction of HAH1 and Wilson protein observed here was not the result of overexpression, because this same result was obtained by utilizing lysates from HepG2 cells endogenously expressing Wilson protein (Fig. 2D). Because considerably less Wilson protein is expressed in HepG2 cells relative to the transfected COS-7 cells (Fig. 2D, lanes 1 and 2), the abundance of Wilson protein signal detected in this experiment was less than that obtained for COS-7 cells (Fig. 2D, lanes 4 and 6). Never-

theless, this interaction was specific, because no Wilson protein was detected with GST alone (Fig. 2D, lanes 3 and 5).

To determine whether the HAH1-Wilson protein interaction occurs *in vivo*, coimmunoprecipitation experiments were performed by using HepG2 cells, which endogenously express both proteins (17). After immunoprecipitation, the immunocomplexes were analyzed by SDS/PAGE, and the presence of either HAH1 or Wilson protein was determined by immunoblotting. As can be seen in Fig. 3A, immunoprecipitation of HepG2 cells with Wilson antisera resulted in detectable HAH1. This association of HAH1 and the Wilson protein was specific and not the result of the washing conditions, because immunoprecipitation with antisera for SOD1 or the copper chaperone CCS did not result in any detectable HAH1 protein. Similarly, when these experiments were repeated by using HAH1 antisera, Wilson protein was consistently detected by immunoblotting (Fig. 3A).

The Wilson and Menkes copper transporters work by common biochemical mechanisms but are differentially expressed in various cell lines and tissues (3). In contrast, HAH1 appears to be ubiquitously expressed. To determine whether the interaction of HAH1 with the Wilson protein reflects a common mechanism for copper trafficking to the secretory pathway of all cells, coimmunoprecipitation experiments were repeated in HeLa cells, which are known to express the Menkes protein (18). Under these circumstances, HAH1 was detected after immuno-

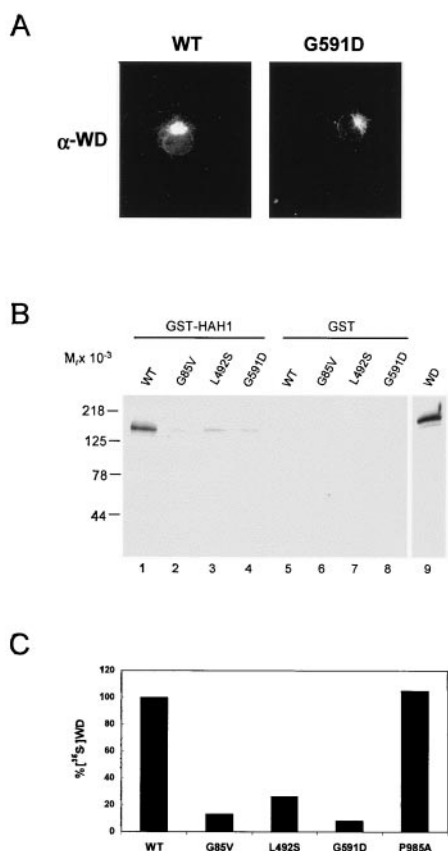


**Fig. 5.** (A) Indirect immunofluorescence of Wilson protein in COS-7 cells transiently transfected with wild type (Left) or G591D mutant (Right). Cells were processed for immunofluorescence 72 hr posttransfection (X60). (B) COS-7 cells expressing either wild-type or mutant Wilson proteins were lysed, incubated with GST-HAH1, and interacting proteins were separated by SDS/PAGE and analyzed by immunoblotting with Wilson antisera. (C) Wild-type and mutant Wilson proteins were translated *in vitro* in the presence of [<sup>35</sup>S]methionine and [<sup>35</sup>S]cysteine, incubated with GST-HAH1, and interacting proteins analyzed by fluorography after SDS/PAGE and were quantitated by PhosphorImager.

precipitation with Menkes antisera (Fig. 3B). The interaction of HAH1 and the Menkes protein was copper dependent, because these same experiments repeated in HeLa cells grown in the presence of BCS failed to detect any HAH1 (Fig. 3B, lanes 3 and 4). A similar copper dependence was also observed for the HAH1–Wilson protein interaction in HepG2 cells (Fig. 3B, lanes 5–8).

Sequence alignment of the six amino-terminal copper-binding domains of Wilson and Menkes proteins reveals considerable homology with HAH1 (Fig. 4A). In addition to the copper-binding MXCXXC motifs, several hydrophobic and charged amino acids are conserved, suggesting that these residues may be involved in stabilizing protein–protein contacts. Because HAH1 interacts with both ATPases in a copper-dependent manner, impairment of this interaction could, in principle, lead to a disruption of cellular copper homeostasis. Although no known disease-associated mutations occur in this region of the Menkes protein, recently such mutations have been identified in patients with Wilson disease (21). Molecular modeling of three of these missense mutations utilizing the NMR solution structure of the fourth copper-binding domain of the Menkes protein indicates the potential of these mutations for disruption of the tertiary structure of this region (Fig. 4B).

To determine whether these mutations effect HAH1–Wilson protein interaction, cDNA constructs containing each mutation were transfected into COS-7 cells and analyzed by using the GST column-binding assay. Immunoblot analysis after transfection revealed equivalent expression of wild-type and mutant Wilson proteins (data not shown). Furthermore, immunofluorescent microscopy revealed the expected trans-Golgi network localization for the wild type and G591D (Fig. 5A), as well as the G85V and L492S mutants (data not shown), suggesting that these mutations do not interfere with the cellular trafficking of the Wilson protein. However, when the amount of protein retained on the GST-HAH1 column was compared with wild-type Wilson protein, all three Wilson mutants showed a marked diminution in HAH1 binding (Fig. 5B). To be certain that these differences were not caused by variations in the level of expression of these proteins in the transfected cells, these studies were repeated by utilizing *in vitro*-translated proteins. When the results were quantitated by using equivalent amounts of [<sup>35</sup>S]-labeled proteins, a consistent and specific decrease in HAH1 binding was detected for all three Wilson disease mutations (Fig. 5C). In contrast, a Wilson disease mutation (P985A) previously shown to affect copper transport through the membrane channel (17) showed no decrease in HAH1 binding in this same assay (Fig. 5C).

## Discussion

Taken together, the data in this study provide a model for the function of HAH1 as a copper chaperone in mammalian cells. The biosynthetic and immunofluorescent studies reveal that HAH1 is synthesized as a single-chain stable protein distributed throughout the cytoplasm and nucleus of cells. The ubiquitous expression of HAH1 is consistent with previous mRNA data and suggests a common function for this protein in all cell types (11). The intracellular copper concentration had no effect on the distribution or stability of HAH1, supporting the concept that vectorial copper transport may be driven by the ATP-dependent thermodynamic gradient established by the Wilson and Menkes proteins (13). In contrast to the nuclear distribution of HAH1 observed in this study, the yeast homologue Atx1p is located only in the cytoplasm (5). Whereas copper has been shown to play a significant role in the regulation of gene expression in yeast, this same process has not been demonstrated in mammalian cells (26). It is therefore possible that the observed differences in nuclear localization of these copper chaperones may reflect fundamental differences in the mechanisms of copper homeostasis in these organisms. Although the digitonin permeabilization studies suggest that the nuclear distribution of HAH1 is determined by diffusion, the considerable lysine content of this protein may play a role in active import of this protein (27).

The Wilson and Menkes proteins are members of a family of P-type ATPases that function to transport copper across intracellular membranes (28, 29). The data in this study demonstrate direct copper-dependent interaction between HAH1 and the Wilson and Menkes proteins *in vitro* and *in vivo*. Taken together with previous studies in yeast, these data support a model for HAH1 function determined by the binding of cellular copper, subsequent trafficking of HAH1-bound copper to the transport ATPases in the trans-Golgi network followed by the transfer of this copper from HAH1 by direct protein interaction. The presumed transient nature of this interaction, predicted by spectroscopic and structural data (13, 14), would permit diffusion-driven movement of cellular copper via the rapid association and dissociation of HAH1 with the ATPases. Such an interaction is consistent with the immunofluorescent data, which reveal no detectable HAH1 concentrated at the trans-Golgi network, and by coimmunoprecipitation studies, which indicate that 3–5% of HAH1 coprecipitate with the ATPases in the presence of copper. The finding that the copper-binding cys-

teines in HAH1 are essential for this interaction is supported by spectroscopic studies that predict a role for these cysteines in Atx1p function via two- and three-coordinate intermediates with the copper-binding domains of Ccc2p (13). This model of HAH1 function would then predict that this protein plays a critical role in monitoring the intracellular concentration of copper. Given recent observations suggesting that under physiologic circumstances little or no free copper exists in the cell, understanding the mechanisms of copper trafficking to HAH1 and the factors that regulate this process will be an important issue for future studies (30).

Comparison of the NMR structure of the fourth copper-binding domain of the Menkes protein with the crystal structure of Atx1p reveals a high degree of structural homology with distinct acidic and basic patches on the respective surfaces of these two proteins (14, 16). On the basis of this observation, it has been proposed that electrostatic interactions, hydrogen bonding, and copper-induced allosteric interactions all play a role in the interaction of this chaperone with Ccc2p (15). Although no disease-associated mutations have been reported in this region of the Menkes protein, three missense mutations (G85V, L492S, and G591D) were identified in the corresponding copper-binding domains of the Wilson protein that result in Wilson disease in multiple affected family members (21). All three missense mutations are in highly conserved regions, implying an essential structural role in these domains (Fig. 4B). The G591 is located in the sixth copper-binding domain and experiments in fibroblasts (32), and yeast (33, 34) have suggested that this region is essential for copper transport and copper-induced trafficking of the Wilson protein. Although previous studies have revealed that several Wilson disease mutations result in defects in protein trafficking (31), expression of these three amino-terminal mutations revealed normal cellular localization (Fig. 5A). However, in support of the interaction model discussed above, the GST-binding analysis with these same mutants revealed a marked impairment in interaction with HAH1. Recently, a missense mutation in *RAN-1* (G173E), the Wilson/Menkes homologue in *Arabidopsis thaliana*, was found to result

in a severely impaired growth phenotype in this organism because of impaired copper delivery to the ethylene receptor, an essential cuproprotein in plants (35, 36). Because *Arabidopsis* also contains a functional Atx1p homologue (9), and the molecular modeling (Fig. 4B) suggests a critical interaction of the glycine residue mutated in *RAN-1* with the leucine mutation in the Wilson protein (L492S) shown here to abrogate HAH1 binding, the data suggest that *RAN-1* mutation may similarly affect copper homeostasis by impairing chaperone-ATPase interaction.

The finding that mutations in the Wilson disease protein abrogate HAH1 binding reveals an essential role for this chaperone in cellular copper homeostasis and provides a mechanism for the development of Wilson disease that is relevant to the pathophysiology and treatment of this disorder. These data suggest that the copper-dependent hepatocyte injury in patients with Wilson disease may be directly related to the ability of HAH1 to bind and traffic excess cytoplasmic copper. Elucidation of the mechanisms of copper delivery to this chaperone from storage sites within the cell may then provide therapeutic approaches to the treatment of copper overload. Although a complete loss of HAH1 would be predicted to result in significant systemic abnormalities in copper homeostasis given the ubiquitous expression of this protein, mutations resulting in diminished function of this chaperone might be predicted to result in impaired homeostasis only in those organs, such as liver and brain, where copper is abundant. This concept then raises the possibility of a role for HAH1 in inherited neurodegenerative disease (37) and the ecogenetic disorders of copper homeostasis such as Indian childhood cirrhosis (38).

We thank Val Culotta and Tom O'Halloran for useful comments and for sharing information before publication, Georgios Loudianos for information regarding the Wilson mutations, Debra Babcock for guidance with the confocal microscopy, and Scott Saunders and Dave Wilson for critical review of the manuscript. These studies were supported by National Institutes of Health grant DK44464 (J.D.G.). J.D.G. is a recipient of the Burroughs Wellcome Scholar Award in Experimental Therapeutics.

- Solomon, E. I. & Lowery, M. D. (1993) *Science* **259**, 1575–1581.
- Harris, Z. L. & Gitlin, J. D. (1996) *Am. J. Clin. Nutr.* **63**, 836S–841S.
- Schaefer, M. & Gitlin, J. D. (1999) *Am. J. Physiol.* **276**, G311–G314.
- Valentine, J. S. & Gralla, E. B. (1997) *Science* **278**, 817–818.
- Lin, S. J. & Culotta, V. C. (1995) *Proc. Natl. Acad. Sci. USA* **92**, 3784–3788.
- Lin, S. J., Pufahl, R. A., Dancis, A., O'Halloran, T. V. & Culotta, V. C. (1997) *J. Biol. Chem.* **272**, 9215–9220.
- Askwith, O., Eide, D., VanHo, A., Bernard, P. S., Li, L., Davis-Kaplan, S., Sipe, D. M. & Kaplan, J. (1994) *Cell* **76**, 403–410.
- Wakabayashi, T., Nakamura, N., Sambongi, Y., Wada, Y., Oka, T. & Futai, M. (1998) *FEBS Lett.* **440**, 141–146.
- Himelblau, E., Mira, H., Lin, S. J., Culotta, V. C., Penarrubia, L. & Amasino, R. M. (1998) *Plant Physiol.* **117**, 1227–1234.
- Culotta, V. C., Linn, S.-J., Schmidt, P., Klomp, L. W. J., Casareno, R. L. B. & Gitlin, J. D. (1999) *Adv. Exp. Biol. Med.* **448**, 247–254.
- Klomp, L. W., Lin, S. J., Yuan, D. S., Klausner, R. D., Culotta, V. C. & Gitlin, J. D. (1997) *J. Biol. Chem.* **272**, 9221–9226.
- Hung, I. H., Casareno, R. L., Labesse, G., Mathews, F. S. & Gitlin, J. D. (1998) *J. Biol. Chem.* **273**, 1749–1754.
- Pufahl, R. A., Singer, C. P., Peariso, K. L., Lin, S. J., Schmidt, P. J., Fahrni, C. J., Culotta, V. C., Penner-Hahn, J. E. & O'Halloran, T. V. (1997) *Science* **278**, 853–856.
- Rosenzweig, A. C., Huffman, D. L., Hou, M. Y., Wernimont, A. K., Pufahl, R. A. & O'Halloran, T. V. (1999) *Structure (London)* **7**, 605–617.
- Portnoy, M. E., Rosenzweig, A. C., Rae, T., Huffman, D. L., O'Halloran, T. V. & Culotta, V. C. (1999) *J. Biol. Chem.* **274**, 15041–15045.
- Gitschier, J., Moffat, B., Reilly, D., Wood, W. I. & Fairbrother, W. J. (1998) *Nat. Struct. Biol.* **5**, 47–54.
- Hung, I. H., Suzuki, M., Yamaguchi, Y., Yuan, D. S., Klausner, R. D. & Gitlin, J. D. (1997) *J. Biol. Chem.* **272**, 21461–21466.
- Yamaguchi, Y., Heiny, M. E., Suzuki, M. & Gitlin, J. D. (1996) *Proc. Natl. Acad. Sci. USA* **93**, 14030–14035.
- Smith, D. B. & Johnson, K. S. (1988) *Gene* **64**, 31–40.
- Olmsted, J. B. (1981) *J. Biol. Chem.* **256**, 11955–11957.
- Loudianos, G., Dessi, V., Lovicu, M., Angius, A., Nurchi, A., Sturniolo, G. C., Marcellini, M., Zancan, L., Bragetti, P., Akar, N., et al. (1998) *Hum. Mutat.* **98**, 640–642.
- Bradford, M. M. (1976) *Anal. Biochem.* **72**, 248–254.
- Casareno, R. L., Waggoner, D. & Gitlin, J. D. (1998) *J. Biol. Chem.* **273**, 23625–23628.
- Petris, M. J., Mercer, J. F. B., Culvenor, J. U. G., Lockhart, P., Gleeson, P. A. & Camakaris, J. (1996) *EMBO J.* **15**, 6084–6095.
- Culotta, V. C., Klomp, L. W. J., Strain, J., Casareno, R. L. B., Krems, B. & Gitlin, J. D. (1997) *J. Biol. Chem.* **272**, 23469–23472.
- Winge, D. R., Jensen, L. T. & Srinivasan, C. (1998) *Curr. Opin. Chem. Biol.* **2**, 216–221.
- Palmeri, D. & Malim, M. H. (1999) *Mol. Cell. Biol.* **19**, 1218–1215.
- Solozio, M. & Vulpe, C. (1996) *Trends Biochem. Sci.* **21**, 237–241.
- Lutsenko, S. & Kaplan, J. H. (1995) *Biochemistry* **34**, 15607–15613.
- Rae, T. D., Schmidt, P. J., Pufahl, R. A., Culotta, V. C. & O'Halloran, T. V. (1999) *Science* **284**, 805–808.
- Payne, A. S., Kelly, E. J. & Gitlin, J. D. (1998) *Proc. Natl. Acad. Sci. USA* **95**, 10854–10859.
- Strausak, D., La Fontaine, S., Hill, J., Firth, S. D., Lockhart, P. J. & Mercer, J. F. (1999) *J. Biol. Chem.* **274**, 11170–11177.
- Forbes, J. R., Hsi, G. & Cox, D. W. (1999) *J. Biol. Chem.* **274**, 12408–12413.
- Payne, A. S. & Gitlin, J. D. (1998) *J. Biol. Chem.* **273**, 3765–3770.
- Hirayama, T., Kieber, J. J., Hirayama, N., Kogan, M., Guzman, P., Nourizadeh, S., Alonso, J. M., Dailey, W., Dancis, A. & Ecker, J. R. (1999) *Cell* **97**, 383–393.
- Rodriguez, F. I., Esch, J. J., Hall, A. E., Binder, B. M., Schaller, G. E. & Bleecker, A. B. (1999) *Science* **283**, 996–998.
- Waggoner, D. J., Bartnikas, T. B. & Gitlin, J. D. (1999) *Neurobiol. Dis.* **6**, 221–230.
- Scheinberg, I. H. & Sternlieb, I. (1996) *Am. J. Clin. Nutr.* **63**, 842S–845S.